^{13}C MRS in Human Tissue

Martin Kršš ák

Medical University of Vienna, Vienna, Austria

This article describes the application of carbon-13 (^{13}C) magnetic resonance spectroscopy (MRS) for the study of human tissue metabolism and pathophysiology. An introduction to the topic, describing technical requirements for nonproton (X) nuclei MRS experiments and methods for increasing the low inherent sensitivity of ^{13}C MRS, is followed by a review of methods and experiments applied to study adipose tissue, skeletal muscle, liver, and brain. Muscle and liver studies focus on the relationship between glucose and glycogen metabolism, exercise physiology, and the development, manifestation, and possible treatment of diabetes mellitus. ^{13}C MRS in the brain has provided a quantitative assessment of neurotransmitter metabolism and neuroenergetics.

Keywords: ^{13}C magnetic resonance spectroscopy, adipose tissue, skeletal muscle, liver, brain, glucose metabolism, lipids, insulin resistance, diabetes mellitus, exercise

How to cite this article:
eMagRes, 2016, Vol 5: 1027–1038. DOI 10.1002/9780470034590.emrstm1490

Introduction

A large spectral dispersion, the presence of carbon nuclei in almost every organic structure, and the nonzero spin of carbon-13 (^{13}C) nuclei have made ^{13}C magnetic resonance (MR) spectroscopy (MRS) well suited for studies of molecular structure and biochemistry in cellular and animal models since the early days of biochemical MRS. The dynamic assessment of biochemical pathways, in particular, forms the basis for the current application of ^{13}C MRS in humans.

Owing to the different magnetic properties of ^{13}C compared to protons (^{1}H, with gyromagnetic ratio $\gamma_{1_H} = 42.476$ MHz/T vs $\gamma_{13_C} = 10.705$ MHz/T), the resonance frequency of ^{13}C at a given magnetic field is approximately one-quarter that of protons. Thus, in addition to the usual clinical settings, an MRS system used for ^{13}C MRS must be equipped with broadband RF electronics (transmitter, RF amplifier, and receiver). In addition, dedicated MR probes are necessary to observe signals that originate from protons, as well as from carbon.

The second consequence of the lower gyromagnetic ratio is the low intrinsic sensitivity of ^{13}C MRS (approximately 1.6% compared to ^{1}H), which in combination with low natural abundance of ^{13}C nuclei (1.1%) hampers the spatial and temporal resolution of ^{13}C MRS experiments. To overcome this problem, a volume of interest of several hundred milliliters is used, frequently by applying localization based on the sensitive volume of RF surface coil. Using this approach, the detection limit in ^{13}C MR spectra is about 20–50 mmol·l tissue^{-1} without artificial enrichment of the observed metabolite pool. Techniques to increase the signal-to-noise ratio (SNR) of ^{13}C MRS include (i) the use of special ^{1}H (decoupling) coils and pulses to eliminate the spin–spin coupling interaction between ^{13}C-nuclei and its surrounding protons; (ii) the use of the ^{1}H–^{13}C interaction with polarization transfer techniques for signal enhancement and/or localization; (iii) the use of a higher field-strength MRS systems; (iv) averaging of the MRS signal using a high number of repetitions; and (vii) increasing the abundance of the ^{13}C isotope by systemic infusion of ^{13}C-labeled metabolites.

Methods

RF Coils

Multichannel RF coils are often used in multinuclear MR experiments. In ^{13}C studies, a ^{13}C channel is typically used for RF transmission and signal reception and a ^{1}H channel is used for scout MRI, shimming, and to decouple ^{1}H–^{13}C interactions and/or provide NOE. To fulfill the latter two functions, there are specific requirements for the ^{1}H channel. In addition to having the best achievable electric decoupling and isolation from the ^{13}C channel, the transverse excitation field (B_1^+) of the ^{1}H channel must be homogeneous and provide adequate intensity over the whole sensitive volume of the ^{13}C coil's volume of interest.

For studies of the calf muscle and the occipital region of the brain, the half-volume 'Adriany' coil[1] fulfills both requirements. A single-channel, linearly polarized planar ^{13}C RF coil (8–10 cm) placed adjacent to the area of interest is, in this case, accompanied by two coil elements that produce a circularly polarized ^{1}H B_1^+ field by adjusting the phase shift between the elements to 90° and thereby provide a fairly homogeneous ^{1}H B_1^+ half-volume within the ^{13}C coil's volume. This geometrical arrangement of both channels also yields an optimal electric isolation of both channels. The carbon channel's sensitivity can be further increased by also using a quadrature coil for the ^{13}C

channel, with resonant traps inserted to facilitate isolation.[2–4] The half-volume ^{1}H/surface coil ^{13}C arrangement can also be reversed if the signal detection on the ^{1}H channel and MRS editing requires a strong and homogeneous B_1^+ on the ^{13}C frequency.[5]

Studies on the liver can use a similar RF coil assembly,[6] with deeper penetration of both ^{13}C and ^{1}H B_1 fields afforded by increasing the dimensions of circular- or butterfly-shaped planar coils. For the investigation of deeper brain structures, a dual-tuned version of the open half-birdcage design that provides more uniform fields at both frequencies has been designed and compared to the above-mentioned coils.[7] Here again, resonant traps at alternate coil legs are used for channel isolation.

Although the interaction of two channels can be reduced by the geometric configuration or the use of resonant traps, the interference between the two coils and the connected RF cables is usually strong enough to pick up significant noise when broadband decoupling is attempted. As decoupling is performed during signal acquisition, even small imperfections can lead directly to degradation of the observed signal. For almost all heteronuclear experiments involving broadband decoupling, it is therefore crucial to apply band-pass filters to the decoupling channel to filter out the frequencies that lead to noise in the observe channel. A more detailed review of RF coils and the hardware setup of ^{13}C MRS experiments can be found elsewhere.[8,9]

^{1}H Decoupling and Processing

Although an increased main static magnetic field strength, B_0, leads to increased sensitivity of the MR experiment, many ^{13}C MRS studies have been performed at $B_0 < 3$ T.[10–13] The disadvantage of the lower sensitivity at such fields is often compensated by efficient broadband ^{1}H decoupling and/or NOE, which is more easily achieved within specific absorption rate (SAR) limits to RF exposure during human experiments. The impact of SAR limits increases with increasing B_0. For decoupling, values over the SAR limit can often be avoided by allowing longer cool-down periods between the pulses (not an option for NOE that requires several spin lattice times T_1 to establish), using longer repetition times (TR), or shorter but efficient RF pulses for the sequence. In this respect, several methods, ranging from the 'classic' and often-used 'WALTZ' or 'MLEV' methods[14,15] to the novel stochastic distribution of ^{1}H-decoupling pulses[16] and combined with more efficient ^{1}H decoupling coils, have been implemented and successfully used at higher fields of 4 and 7 T.[4,17–19]

Despite technical challenges, the excellent spectral dispersion of ^{13}C MRS and the lack of an intense and complex natural ^{13}C MRS background permit rather simple spectral processing and quantitation. In contrast to ^{1}H MRS, where sophisticated methods of spectral deconvolution are necessary, simple signal integration or line-fitting in the frequency domain is often accurate and robust enough for ^{13}C MRS quantification. Different approaches have been used to convert the signal intensity into molar concentrations, but the method of comparing the in vivo MRS signal to that of an external phantom solution with known concentration as a reference[20,21] is used most frequently.

Applications: Tissue Lipid Profiling and Assessment

The most accessible and straightforward application of ^{13}C MRS is in the assessment of the lipid profile from the strong naturally abundant lipid signal that arises from adipose tissue. Early studies were able to assess adipose tissue lipid composition in malnourished patients following liver transplantation,[22] and in neonates.[23] One study used a simple pulse-and-acquire, proton-decoupled ^{13}C MRS sequence to demonstrate differences in the double-bond distribution (Figure 1) of adipose tissue lipids that were caused by diets that contained predominantly polyunsaturated fatty acids (FA) and monounsaturated FA.[24] Nonlocalized, proton-decoupled ^{13}C MRS of adipose tissue also detected the signal from trans-FA ingested in a Western style diet.[25]

The natural abundance of the ^{13}C isotope delivers sufficient SNR for the assessment of muscle and liver triglyceride content. Perseghin *et al.*[26] studied the relation between muscle triglyceride levels and insulin resistance, a major predictor of the onset of type 2 diabetes. Petersen *et al.*[27] applied the method to assess hepatic lipid content in patients with hepatitis. Recently,

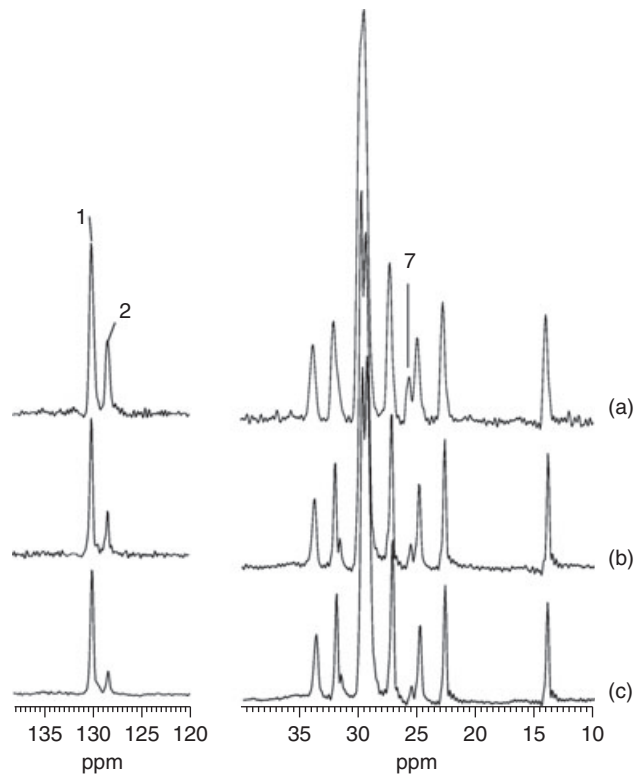

Figure 1. Natural abundance ^{13}C spectra (1.5 T) of adipose tissue depicting the effect of long-term diets containing different fraction of polyunsaturated fatty acids (PUFAs) and monounsaturated fatty acids (MUFAs). The changes in PUFA levels are clearly delineated in peak 2 (128 ppm CH=CH–CH_2–CH=CH–) and 7 (25.5 ppm CH_2=CH–CH_2–CH=CH_2: diallylic or bisallylic in PUFA) in response to diets. (a) Spectrum from subject on PUFA (fish oil) diet for >7 years. (b) Spectrum from a control subject. (c) Spectrum from a subject on MUFA diet for 8 years. (Reproduced with permission from Ref. 24. © John Wiley & Sons, Ltd., 2003)

heteronuclear (^{1}H–^{13}C) editing methods have demonstrated increased sensitivity for detecting the ratio of saturated to unsaturated lipids in human skeletal muscle[28] and measuring ^{13}C-labeled lipid uptake in skeletal muscle and liver in animal models of diabetes.[29] All of these studies demonstrate the ability to discriminate lipid ^{13}C MRS signals in adipose tissue, liver, and skeletal muscle with sufficient SNR using currently available MRS hardware and data-acquisition schemes.

Skeletal Muscle Metabolism

Natural Abundance and Labeling

The in vivo measurement of tissue glycogen concentration was enabled by the discovery that ^{13}C MRS could visualize glycogen in skeletal muscle and liver in animal models in vivo.[30–32] This was later validated in several studies on rabbit liver[20] and human skeletal muscle.[21] Despite its high molecular weight, the glycogen C-1 resonance is 100% visible[31,33] owing to the high intramolecular mobility of its moieties. Skeletal muscle glycogen is present at approximately 80–120 mM concentrations, depending on the muscle and physiological conditions.[34–36] Good reproducibility of natural abundance ^{13}C MRS glycogen measurements[37] has allowed the use of experimental protocols that assess glycogen depletion during exercise and subsequent recovery (Figure 2),[12,35,38–40] as well as glycogen reduction in nonexercising muscle.[12]

An infusion of ^{13}C-labeled glucose as a substrate can, under steady-state conditions, increase the accuracy of measurements of glycogen synthesis.[41] Indeed, glycogen synthesis in skeletal gastrocnemius muscle has been quantified (Figure 3)[42] and correlated with whole-body carbohydrate consumption.[43] By combining in vivo ^{13}C, phosphorus (^{31}P) MRS, and microdialysis in a single experiment in which ^{13}C-labeled glucose and ^{13}C-labeled mannitol are infused intravenously as a substrate and a marker for extracellular volume, respectively, the intracellular free glucose concentration can be quantified. For quantification, the creatine ^{13}C MRS signal is used to measure intracellular volume and the glucose-6-phosphate concentration measured from the phosphorus (^{31}P) MRS signal is subtracted from the ^{13}C-labeled glucose signal.[44,45] This and another ^{13}C MRS method[46–48] have found that the defect in the transport of glucose into the muscle cell precedes defects in phosphorylation and glycogen synthesis in patients with type 2 diabetes mellitus (T2DM),[45] thus identifying a potentially important step in the development of insulin resistance.

The labeling of substrates in the tricarboxylic acid cycle (TCA) by infusing [2-^{13}C]-labeled acetate and observing the enrichment of the C4 position of glutamate has been performed in muscle to measure mitochondrial activity. The flux through the TCA cycle is a surrogate for the rate of mitochondrial oxygen consumption by the cellular respiratory apparatus. These measurements can easily be combined with experiments in which undirectional flux through the skeletal muscle adenosine triphosphate (ATP) synthase is measured by means of saturation transfer (see ***Measuring Biochemical Reaction Rates In Vivo with Magnetization Transfer***). This latter method measures the flux of inorganic phosphate (Pi) involved in ATP synthesis, by magnetically labeling the γ-phosphorus position of ATP in skeletal muscle and quantifying the corresponding decrease in the Pi pool.[49,50] In accordance with previous results, these MRS studies found that the mitochondrial oxidative and phosphorylation activity of skeletal muscle is associated with a decrease in peripheral insulin sensitivity and an increased intramyocellular lipid content in both elderly sedentary individuals[50] and insulin-resistant offspring of T2DM patients.[51]

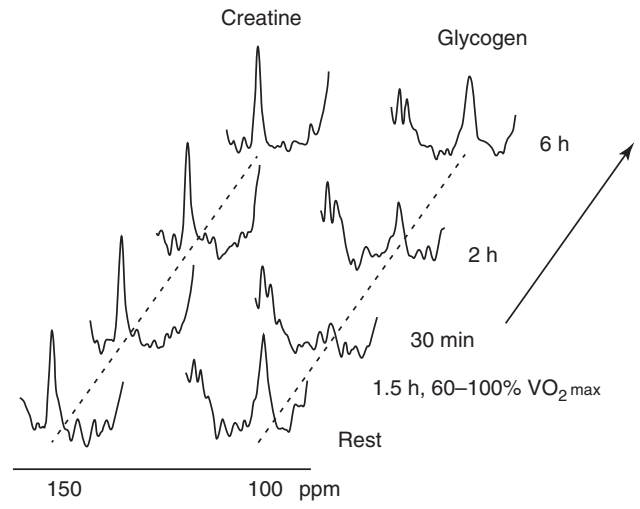

Figure 2. Natural abundance ^{13}C spectra (1.5 T) showing creatine and glycogen peaks from quadriceps muscle of a single subject as a function time during an exercise protocol. Creatine is used as an internal reference because it remains stable in exercise and recovery. The glycogen signal is decreased after exercise on bicycle ergometer and increases with time after ingestion of a carbohydrate-loaded drink. (Reproduced from Springer, Magma: Magnetic Resonance Materials in Physics, Biology, and Medicine, Muscle glycogen recovery after exercise measured by ^{13}C-magnetic resonance spectroscopy in humans: effect of nutritional solutions, 11, 2000, 114–121, S. Rotman, J. Slotboom, R. Kreis, C. Boesch, E. Jéquier © With permission of Springer Science+Business Media)

Insulin Resistance, T2DM, and Substrate Overabundance

Many ^{13}C MRS studies employing simple pulse-and-acquire sequences have characterized the defects in skeletal muscle metabolism in insulin-resistant states, including experimental manipulations. These studies revealed a ~60% decrease of insulin-stimulated glycogen synthesis in overt T2DM patients,[43] as well as a comparable impairment in their lean insulin-resistant offspring[35,52] and in obese nondiabetic insulin-resistant volunteers.[53] Similar ^{13}C MRS approaches have shown decreased postprandial skeletal muscle glycogen synthesis under normal physiologic conditions after a standard carbohydrate-rich breakfast and lunch in T2DM patients.[36]

Combinations of pulse-and-acquire ^{13}C and ^{31}P MRS methods have also been used to monitor the effect of life-style changes and pharmacological insulin-sensitizing therapy on skeletal muscle glucose metabolism. One bout of aerobic exercise normalized insulin-stimulated glucose fluxes along with the normalization of whole-body insulin sensitivity in

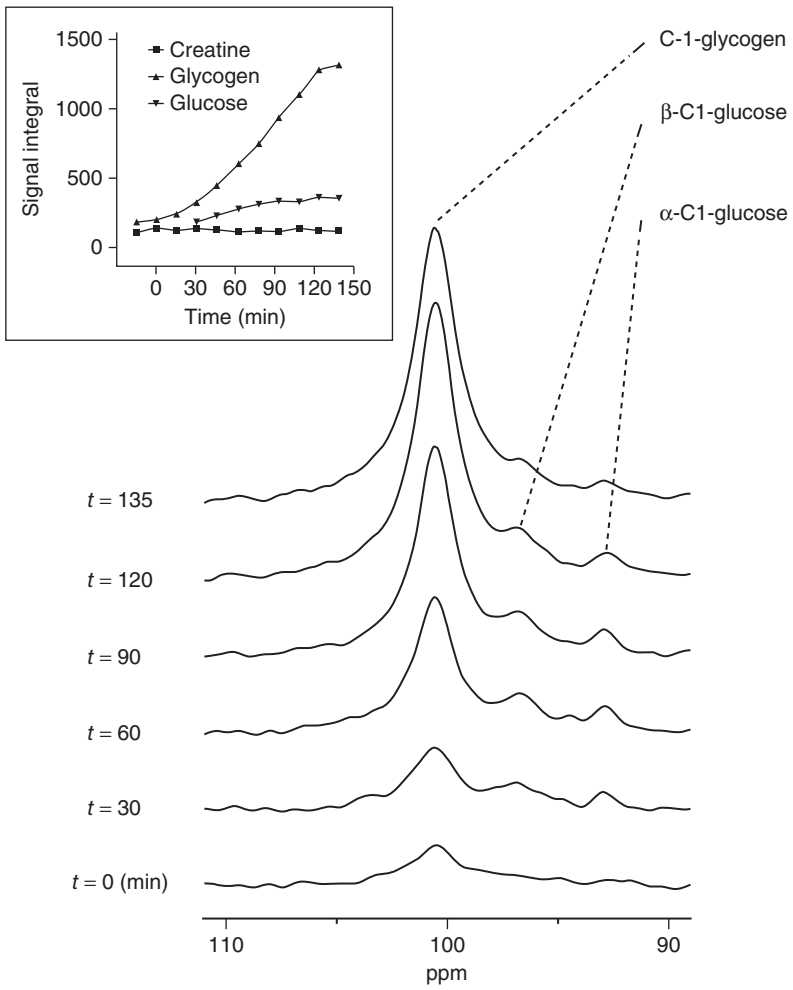

Figure 3. In vivo ^{13}C spectra recorded from the human calf muscle at 1.5 T under euglycemic-hyperinsulinemic conditions. The spectrum at the bottom shows the natural abundance C-1 signal of glycogen at 100 ppm. During the glucose infusion, signals from both glucose anomers are clearly visible. The strong increase in the C-1 signal of glycogen over time reflects the incorporation of labeled glucose. The insert shows the integrated values of the fitted signals from creatine, glycogen, and glucose over time. (Reproduced with permission from Ref. 42. © John Wiley & Sons, Ltd., 2000)

insulin-resistant offspring of T2DM patients,[54] while troglitazone treatment improved the skeletal muscle glucose transport and the glycogen metabolism of patients with T2DM.[42,55]

The role of free fatty acids (FFA) and amino acids (AAs) in skeletal muscle glucose metabolism has been investigated in several studies that simulated the metabolic conditions of T2DM in young healthy men. An experimentally induced increase in plasma FA concentrations showed that substrate overabundance decreased glucose transport and phosphorylation[56–58] and impaired skeletal muscle glycogen synthesis,[58] which preceded the decrease in whole-body glucose uptake in a dose-dependent manner.[57] The observed effect of over-abundance also holds true in various conditions of insulinemia,[56–58] as well as with depleted skeletal muscle glycogen.[59] Measuring skeletal glucose transport/phosphorylation and glycogen synthesis in the skeletal muscle of young healthy men during an experimental AA challenge showed a direct effect of AAs on glucose transport or phosphorylation[60] and reduced skeletal muscle glycogen synthesis. Substrate overabundance and defects in lipid oxidation can lead to increased lipid accumulation inside the skeletal muscle.

Multinuclear MRS studies have also revealed a link between intramyocellular lipid accumulation and skeletal muscle glucose metabolism,[26,61,62] which has also been studied in different states of insulin resistance and physical fitness.[63] This complex issue is discussed, together with hepatic and adipose fat accumulation, elsewhere (see ***Muscle studies by ^{1}H MRS***; ***Body Fat MRS***; ***Insulin resistance, type 2 diabetes and obesity and other metabolic disorders studied by MRS***). In addition, different MR-based approaches to the assessment of skeletal muscle morphology, physiology, and metabolism have been extensively reviewed.[64]

Summarizing the knowledge gained from skeletal muscle nonproton (X)-nuclei studies, we can say that the combination of ^{13}C and ^{31}P MRS: (i) can measure glycogen metabolism and glycogenic substrate flux in human skeletal muscle under various conditions; (ii) has helped uncover defects in this pathway in insulin-resistant conditions; and (iii) has helped discover

links between defects in mitochondrial activity/capacity and lipid metabolism, as well as defects in whole-body and/or skeletal muscle glucose metabolism.

Liver Metabolism

Natural Abundance and Labeling

Hepatic glucose fluxes play a pivotal role in the ability of the liver to store glycogen and maintain normal glucose homeostasis by releasing glucose equivalents from the glycogen stores into the circulation through a process called *glycogenolysis*. In addition, hepatocytes contribute to glucose production by taking up lactate, glycerol, and AAs and converting these substrates into glucose by gluconeogenesis. The simultaneous nature of these processes presents an additional methodological obstacle. As a result, before MR, the relative contributions of gluconeogenesis and glycogenolysis to glucose production in humans were unknown. Another important metabolic pathway observable in the hepatic tissue is the TCA cycle, which releases energy for oxidative ATP synthesis and yields metabolically substantial pools of glutamine and glutamate.

Similar to the situation in muscle, the low natural abundance of the ^{13}C isotope does not preclude the measurement of hepatic glycogen[13,20] with test–retest variability similar to measurements in skeletal muscle.[37] Healthy liver usually presents with a glycogen concentration in the range 180–400 mmol·l^{-1} wet tissue volume, and this large relatively homogeneous tissue positioned close to the body surface can easily be examined with ^{13}C MRS by an appropriate choice of surface RF coils. Hepatocytes, which primarily account for glycogen metabolism, are distributed isotropically and represent ~80% of the parenchymal volume of the liver. Potential contamination of the MRS signal from the abdominal muscles, subcutaneous fat layers, and rib cage can be eliminated by suitable localization techniques. Traditionally, one-dimensional (1-D) inversion-based techniques suppress unwanted overlying signals from muscle and fat layers[13] or 1-D chemical shift imaging (CSI) techniques are used to select only the liver-specific MRS signal.[65] Both these techniques can be applied for noninvasive and repetitive measurements of hepatic glycogen concentrations in a more-or-less 'real-time' mode, which enables the calculation of rates of net glycogen synthesis and glycogenolysis in vivo.

In addition to the quantification of naturally abundant ^{13}C glycogen, tracing ^{13}C label incorporation into glycogen during the infusion or ingestion of [1-^{13}C]-enriched glucose (10–99%) can increase the sensitivity of the method by up to 100-fold. Sequential infusions of ^{13}C-enriched and unlabeled glucose, in the so-called ^{13}C pulse–^{12}C chase experiments,[66] allow the assessment of rates of glycogen synthesis and simultaneous glycogenolysis in humans.[67–70] In these experiments, the increase in total hepatic glycogen during the infusion of [1-^{13}C] glucose over time yields the flux through glycogen synthase. For the estimation of simultaneous glycogenolysis, the change in the [1-^{13}C]glycogen concentration is compared with the predicted increment during the infusion of unlabeled glucose. Here again, constant flux through glycogen synthase is assumed. The difference between the predicted and observed glycogen concentrations provides a minimum estimate of simultaneous glycogenolysis, that is, only the glycogen that is broken down and escapes the hexose-1-phosphate pool.

In a pioneering study by Rothman *et al.*,[13] hepatic glucose fluxes have been monitored and quantified by a combination of ^{13}C MRS to measure glycogen concentration, MRI to measure liver volume, and the infusion of [3-^{3}H]glucose to determine glucose production over a period of 68 h of fasting. Initially, liver glycogen decreases almost linearly at a rate of ~4.3 μmol kg wet tissue^{-1} min^{-1} was observed, with hepatic glycogen reaching a concentration of ~250 mmol l wet tissue^{-1} after 15 h of fasting. This fasting concentration was in agreement with that of ~270 mmol l wet tissue^{-1} obtained by needle biopsy[71] and was also confirmed by another group employing ^{13}C NMR spectroscopy.[10] A later study by Petersen *et al.*,[72] which quantified the contribution of glycogenolysis to glucose production in the first 5–12 h of an overnight fast that followed a large 1000-kcal mixed meal, confirmed these results. That study showed that net hepatic glycogenolysis contributed only about 45% of the whole-body glucose production, implying that gluconeogenesis typically contributes about 50% to the rate of whole-body glucose metabolism during the early hours following a regular meal.

Studies in postprandial states showed that ingestion of a mixed meal resulted in a net rate of glycogen accumulation of ~0.8 mmol l of liver tissue^{-1} min^{-1} under glycogen-depleted conditions,[13] and 0.34–0.38 mmol l liver^{-1} min^{-1} after breakfast or dinner.[73,74] It could be calculated that ~20% of the glucose from the meal was deposited as glycogen in the liver. A study by Hwang *et al.*,[75] which examined changes in hepatic glycogen content following normal eating behavior in nondiabetic subjects, observed a steady step-wise increase in hepatic glycogen stores, indicating negligible hepatic glycogenolysis during a typical day in which meals are ingested approximately 5 h apart. Thus, glucose absorption from meals and gluconeogenesis account for the major part of whole-body glucose appearance during the day, while net hepatic glycogenolysis typically contributes to whole-body glucose production only during the night-time period.

Recently, further metabolic fluxes and the response to oxidative stress in the liver have been reported in vivo. Labeling the hepatic metabolism by infusing [1-^{13}C]-acetate enables the assessment of TCA- and anaplerotic flux (Figure 4). As noted earlier, TCA labeling with [2-^{13}C]-acetate in muscle results in enhancement of the C4 position of glutamate.[49] However, in hepatic tissue, the large amount of lipids will typically obscure the spectral contribution from C4-glutamate and require a different approach to flux labeling and modeling. With the label at the 1-^{13}C position on acetate, the TCA cycle incorporates it into the C5 and C1 positions of glutamate, enabling assessment and quantification of TCA- and anaplerotic fluxes in hepatocytes.[6]

The assessment of hepatic tissue response to oxidative stress is based on the observation of glutathione synthesis. As glutathione is a tripeptide consisting of glycine, cysteine, and glutamate, marking any of the precursors by ^{13}C should result in an increase in the label in the ^{13}C MRS-visible glutathione pool. Recent studies have been able to confirm this in experimental protocols that included infusion and/or ingestion of [2-^{13}C]-glycine in animals and also in humans. By translating the model

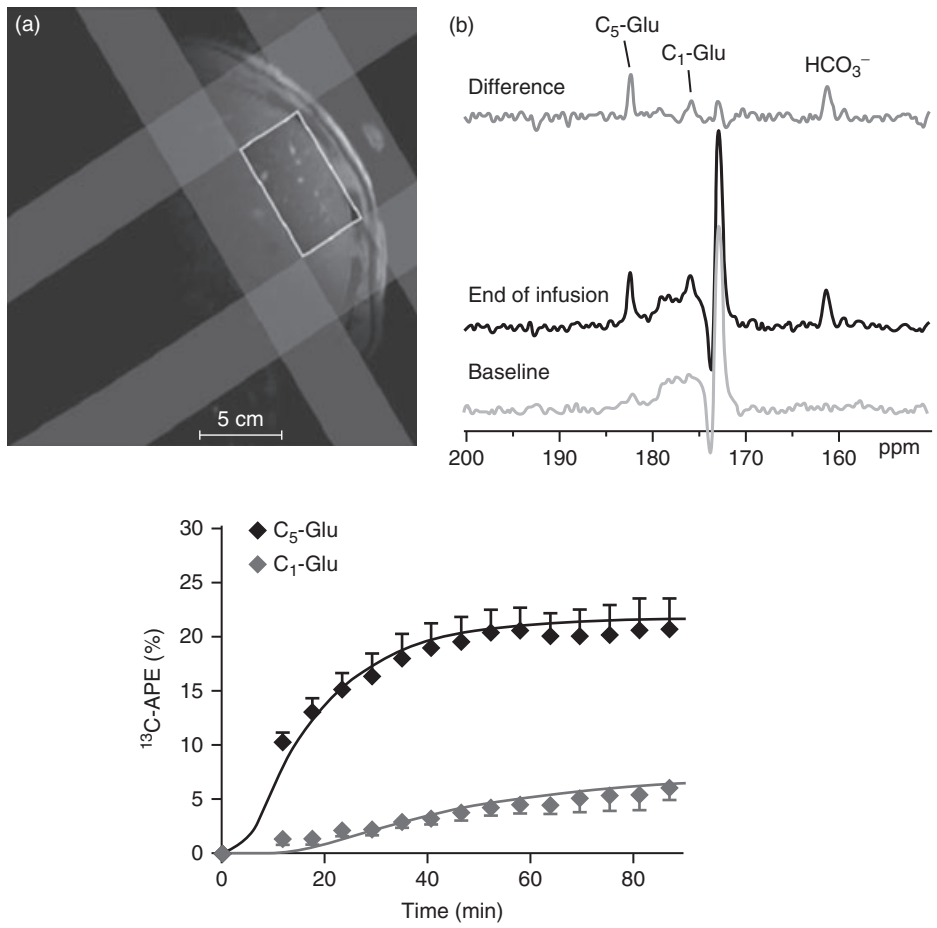

Figure 4. In vivo ^{13}C MRS of the human liver at 4 T. (a) Axial gradient-echo image of the torso acquired during a single breath-hold. ^{1}H-decoupled ^{13}C spectra were acquired from a localized region within the liver. The voxel was selected using outer volume suppression (shaded regions) applied in three dimensions to suppress signals arising from outside the voxel to define a volume of interest (white box). (b) Localized ^{13}C spectra of the human liver acquired before and at the end of a 120-min infusion of [1-^{13}C]acetate. ^{13}C labeling at the C_5 position of glutamate (C_5-Glu) was observed owing to the oxidation of [1-^{13}C]acetate via the TCA cycle. Labeling of glutamate C_1 (C_1-Glu) and the bicarbonate (HCO_3^-) pool was also observed as the ^{13}C label traversed a second turn of the TCA cycle. The lower panel shows time courses of hepatic glutamate C_5 and C_1 enrichment as determined by localized in vivo ^{13}C MRS during infusion of [1-^{13}C]acetate ($n = 12$). The kinetics of liver glutamate enrichment for each subject were determined, based on a metabolic model of hepatic metabolism. The average fit of the model to the glutamate enrichment data is superimposed. Data are expressed as means ± standard errors of the mean. (Reproduced by permission from Macmillan Publishers Ltd: Nat Med, Befroy, D. E.; Perry, R. J.; Jain, N.; Dufour, S.; Cline, G. W.; Trimmer, J. K.; Brosnan, J.; Rothman, D. L.; Petersen, K. F.; Shulman, G. I., Direct assessment of hepatic mitochondrial oxidative and anaplerotic fluxes in humans using dynamic C magnetic resonance spectroscopy, Nat Med 2013. © 2013)

of glycine to glutathione labeling from studies on neoplastic lesions,[76] Skamarauskas *et al.*[77] were able to quantify the rate of glutathione synthesis in rats under conditions of acute and chronic oxidative stress, specifically showing increased rates of synthesis following CCl_4 insult.

A proof-of-concept study in humans used oral ingestion of multiple doses of labeled [2-^{13}C]-glycine, which delivered label to the liver via the portal vein. Even this discontinuous delivery approach led to stable isotope enrichment in the plasma that was sufficient for labeling the glutathione pool in the liver within 8 h of the experimental protocol. Quantitative analysis showed that the variability of the glutathione synthesis rate constant was comparable to the prior experimental studies, focusing on noninvasive assessment of the rate constants of hepatic glycogen metabolism.[67]

Metabolic Syndrome, T2DM, Hormonal Regulation, and Substrates

Studies using ^{13}C MRS to assess hepatic glucose fluxes have focused on the characterization of pathologic conditions, such as T2DM or type 1 diabetes (T1DM), and revealed significant alterations of hepatic glycogen storage, glycogen release, and gluconeogenesis in both patient groups.[67,73,78–81] A defect in the hepatic glycogen storage was also observed in glucokinase-deficient, mature-onset diabetes of young-2 (MODY-2) patients.[82] Lower glycogen synthesis[67,78,79] and unsatisfactory suppression of endogenous glucose production[67,81,83] contribute to postprandial hyperglycemia in diabetes mellitus, and increased gluconeogenesis is the key to postabsorptive hyperglycemia in T2DM.[80] Therapeutic interventions by metformin in T2DM[80] or by insulin have

been used to maintain near-normal glycemia levels in T1DM over the long term[78] and at least partially eliminate or compensate for the defects in glycogen synthesis and/or gluconeogenesis.

Enzymes involved in glycogen metabolism are greatly affected by hormones such as insulin and glucagon. As shown in the [1-^{13}C]-labeled glucose-[1-^{12}C] glucose chase experiment with the concurrent assessment of hepatic glycogen concentration by ^{13}C MRS in healthy humans, the rate of hepatic glycogen synthesis depends on portal vein insulin, which promotes hepatic glycogen cycling.[70,72] Small changes in portal vein concentrations of insulin and glucagon independently affect hepatic glycogen synthesis and glycogenolysis.[70] To assess this effect and possible therapeutic approaches, experiments designed to measure both glycogen cycling and hepatic glucose production were applied in a population with T2DM.

Like in skeletal muscle, the over-abundance of substrates influences hepatic metabolic fluxes.[67,80] Here again, studies in young healthy volunteers have shown that experimentally elevated FFA concentrations increased gluconeogenesis,[84] which then led to a lower rate of hepatic glycogen breakdown.[85] However, matching insulin, glucagon, glucose, and FFA concentrations during a hyperglycemic clamp protocol in T2DM[67] did not fully restore hepatic glycogen synthesis.

Studies focusing on the effect of AAs on hepatic glucose fluxes have shown that experimental AA elevation does not affect hepatic glycogenolysis, but instead increases gluconeogenesis, resulting in an increase in total endogenous glucose production.[86] In recent years, the relationship between hepatic fat accumulation and whole-body (as well as hepatic) glucose fluxes has also been investigated in detail.[74] This issue, together with muscle and adipose fat accumulation, is discussed elsewhere (see ***Body Fat MRS***; ***Monitoring Fatty Liver***; ***Insulin resistance, type 2 diabetes and obesity and other metabolic disorders studied by MRS***; ***In Vivo MRS of Lipids in Adipose Tissue, Bone Marrow, and Liver***).

In summary, ^{13}C MRS is uniquely able to quantify hepatic glycogen synthesis, glycogenolysis, TCA cycle flux, and the response to oxidative stress. Thus, in combination with stable isotope dilution techniques, it has helped to noninvasively assess hepatic glucose fluxes in healthy liver under various conditions. On the basis of the ^{13}C MRS studies of healthy liver, experiments in diabetic patients have revealed the crucial role of defects of hepatic glycogen accumulation and the lack of suppression of glucose production during postprandial and fasting hyperglycemia in both T1DM and T2DM. These studies have also characterized the role of substrate over-abundance and hormonal regulation in the development of these defects. MRS experiments can also be used to investigate therapeutic interventions that target hepatic glucose metabolism in both T1DM and T2DM. In the future, a combination of different MRS-based techniques in a single experiment could be useful for linking steady-state metabolite concentrations to dynamic measures of normal and pathophysiological hepatic metabolism. ^{1}H and ^{31}P MRS have been employed to quantify hepatic lipid content and characterize hepatic tissue in diffuse pathologies of the liver, including in nonalcoholic fatty liver disease, cirrhosis, hepatitis, and T2DM. The connection to whole-body fat compartmentation has also been highlighted (see ***Body Fat MRS***; ***Monitoring Fatty Liver***; ***Insulin resistance, type 2 diabetes and obesity and other metabolic disorders studied by MRS***; ***In Vivo MRS of Lipids in Adipose Tissue, Bone Marrow, and Liver***).

Brain

As in liver and muscle, glucose transport, storage, and metabolism can be deduced from ^{13}C MRS of intact brain tissue. Nevertheless, the biochemistry and physiology of neurotransmitter cycling (glutamine, glutamate, and GABA) have become more important for neurochemical ^{13}C MRS applications.[87–89] Here, the issues of sensitivity, volumes of interest, and the time resolution of the experiments play an even more important role than in liver and muscle studies. A practical guide for ^{13}C MRS data acquisition can be found in the reviews by de Graaf *et al.*[90,91] and Gruetter *et al.*[8]

Direct ^{1}H MRS measurements of brain glucose[92,93] during controlled hyperglycemia have demonstrated increased transport of glucose between plasma and brain tissue in patients with T1DM who were unaware of hypoglycemia. These studies were based on previous results, in which a linear relationship between plasma and brain glucose was established and validated.[94–96] In addition to increased glucose transport, in vivo studies in the rat brain suggest that some mechanism of hypoglycemia-induced brain glycogen overcompensation may exist to protect brain tissue from acute energy shortage during hypoglycemia.[97–99] To quantify brain tissue glycogen, these measurements utilized a robust ^{13}C MRS signal localization technique that combined outer volume suppression and FID signal acquisition.[97,100] This technique was validated by comparison with biochemical measurements.[101] The first study in the human brain[102] confirmed that brain glycogen stores exceed those of free glucose and that brain glycogen metabolism is very slow under normal conditions.

Further downstream of the metabolic pathway, the fluxes in the glutamate/glutamine neurotransmitter cycle, which are critical for normal brain function, have been measured in several studies on healthy volunteers. This work has been comprehensively reviewed by de Graaf, Rothman, and Shulman.[90,103,104]

Using ^{13}C MRS measurements to track the fate of ^{13}C-labeled glucose into the glutamine and glutamate pools in neurons and glia,[105–107] the neuronal and astroglial TCA cycle rates, as well as that of anaplerotic glutamine synthesis, have been quantified. Most of these studies have been performed on MRS systems with $B_0 > 2$ T under steady-state physiologic conditions as well as with steady-state ^{13}C isotopic enrichment of blood plasma controlled via a glucose clamp[105–107] (Figure 5). However, a clinical approach using a simple infusion of [1-^{13}C]glucose[109,110] and/or a [1-^{13}C]acetate solution[111] implemented on a widely available 1.5 T MR system has also successfully characterized brain glucose metabolism[110,112,113] and astroglial TCA cycle flux.[111]

Using the latter simpler approach, with robust pulse-and-acquire signal localization, abnormalities in the ^{13}C enrichment pattern of brain metabolites have been observed in pediatric

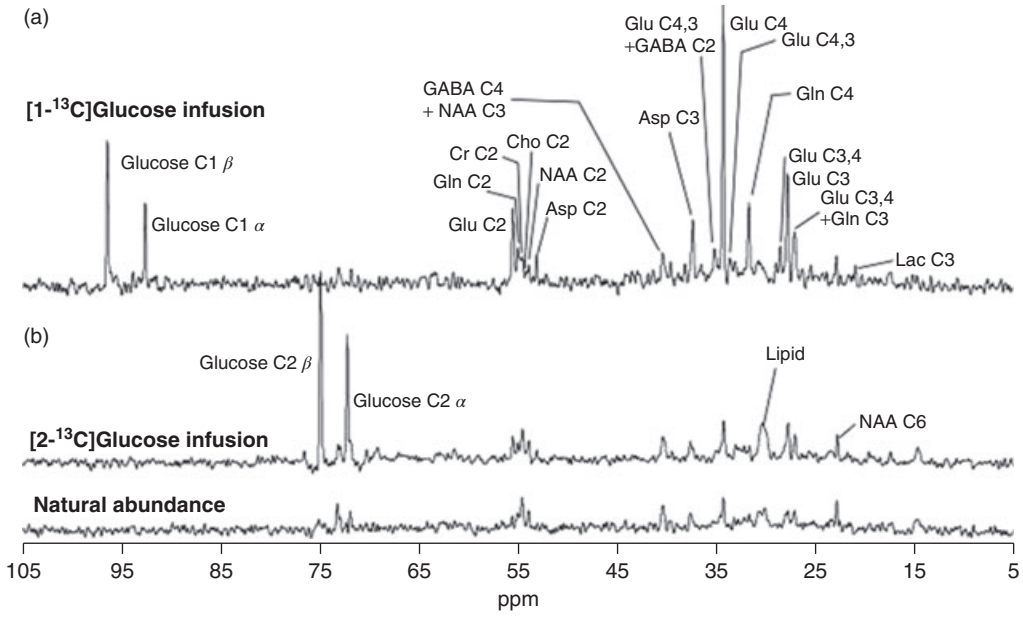

Figure 5. ^{13}C spectra obtained at 2.1 T MR system in the healthy volunteer using either [1-^{13}C]glucose (a) or [2-^{13}C]glucose (b) infusions. Despite having 15% greater plasma glucose enrichment, the data obtained with C2-labeled glucose show that the flux through pyruvate carboxylase is on the order of 10-fold less than that through pyruvate dehydrogenase. The very low labeling of the C4 of glutamate and glutamine might have arisen from pyruvate recycling wherein malate is converted to pyruvate by malic enzyme. This is consistent with much of the anaplerotic flow being devoted to replacing neuronal glutamate lost owing to astroglial oxidation. The small amount of C4 labeling could also arise from transfer of the label from the C2 of glucose to the C1 or the C6 of glucose by pentose phosphate metabolism in the brain or by hepatic gluconeogenesis. (Reproduced with permission from Ref. 108. © John Wiley & Sons, Ltd., 2007)

patients with leukodystrophies and mitochondrial disorders[109] and with disturbed neurotransmitter glutamate/glutamine cycling in chronic hepatic encephalopathy.[112] Although direct ^{13}C MRS provides excellent spectral resolution that enables detailed analysis of the ^{13}C enrichment process, its inherent low sensitivity limits the signal detection to relatively large volumes. Several combined ^{1}H-^{13}C MRS techniques that take advantage of magnetization transfer between highly abundant and highly sensitive protons and between ^{13}C nuclei in specific ^{13}C-labeled chemical bonds have provided tissue-specific localization in neurotransmitter studies.[105–107,114–117] Application of such approaches in functional studies has enabled measurements of TCA cycle activity in the healthy cortex during visual stimulation.[114,118] Both of these studies provide evidence of an almost 50% increase in oxidative glucose consumption in the visual cortex during activation.

In summary, most ^{13}C MRS studies of the brain have focused on the quantitative assessment of neurotransmitter metabolism and neuroenergetics in basal and stimulated conditions. ^{13}C MRS experiments have also played an important role in delineating the role of alternative substrates, such as acetate, ketone bodies, and lactate, in support of neuronal and astrocyte energetics.

Conclusion

Modern in vivo methods of ^{13}C MRS open a window into skeletal muscle and hepatic glucose uptake and homeostasis in living tissue, as well as into skeletal muscle mitochondrial activity. Such studies have been able to quantify defects of glucose metabolism in both skeletal muscle and liver. This knowledge is helping to define the phenotype of the metabolic syndrome, as well as T2DM and T1DM. Carbon-13 MRS measurements enable the monitoring of the response to therapies designed to provoke insulin sensitization and/or lipid reduction. In addition, repetitive ^{13}C MRS measurements have been successfully applied in the field of sports physiology and have increased our knowledge of skeletal muscle glycogen metabolism during exercise and subsequent recovery. In brain tissue, pilot studies suggest that there are protective, over-compensating mechanisms of glycogen storage in the brains of diabetic patients. However, the major application of ^{13}C MRS in brain is to quantify neurotransmitter metabolism and neuroenergetics.

From a technical viewpoint, the major hurdles to applying of ^{13}C MRS to the study of human pathophysiology are the costs, which require ^{13}C substrate infusions and monitoring; RF power deposition during decoupling; the inherent low sensitivity of ^{13}C MRS; and the lack of a technical capability to perform ^{13}C MRS on most clinical MRI/MRS systems. Despite these obstacles, ^{13}C MRS has been successfully applied in studies of diabetes and healthy aging, as well as to a variety of neurological and psychiatric diseases. The increasing availability of high-field MR systems, indirect ^{1}H–^{13}C methods for increased sensitivity, and the development of hyperpolarized ^{13}C (see ***Magnetic Resonance Spectroscopy of Prostate Cancer***; ***Hyperpolarization Methods for MRS***; ***Integration of ^{13}C Isotopomer Methods and Hyperpolarization Provides a Comprehensive Picture of Metabolism***) have the potential

to greatly increase the sensitivity of the method and thereby facilitate future applications of ^{13}C MRS for metabolic imaging in human tissue. These technological developments, together with improvements in ^{13}C infusion protocols, should lead to increased time resolution of dynamic studies that will minimize patient time in the magnet and thus increase the value of ^{13}C MRS to clinical and research studies.

Biographical Sketch

Martin Kršśák, b. 1969. MSc 1992, Bratislava, PhD, 2000, Vienna. Martin first became involved with NMR upon joining the Department of Medical Physics, at the University of Vienna in 1993, using it to characterize liver tissue during experimental transplantation. Subsequently, in 1996, Martin joined the Departments of Internal Medicine and Radiology and contributed to numerous studies on the assessment of metabolism and pathophysiology of type 2 diabetes mellitus using dynamic multinuclear MRS. He has approximately 90 peer-reviewed papers, reviews, and book chapters. His research interests include the assessment of fat distributions and energy metabolism in human skeletal muscle, liver, and heart with multinuclear MRS and MRI.

Related Articles

Detection coils for MRS; Quantifying Metabolite Ratios and Concentrations by Non-^{1}H MRS; Spectral editing in MRS; Muscle studies by ^{1}H MRS; Muscle Studies by ^{31}P MRS; Body Fat MRS; Monitoring Fatty Liver; Insulin resistance, type 2 diabetes and obesity and other metabolic disorders studied by MRS; In Vivo MRS of Lipids in Adipose Tissue, Bone Marrow, and Liver; Hyperpolarized Carbon-13 MRI and MRS Studies

References

1. G. Adriany and R. Gruetter, *J. Magn. Reson.*, 1997, **125**, 178.
2. D. W. Klomp, W. K. Renema, M.van der Graaf, B. E.de Galan, A. P. Kentgens, and A. Heerschap, *Magn. Reson. Med.*, 2006, **55**, 271.
3. M. Meyerspeer, E. S. Roig, R. Gruetter, and A. W. Magill, *Magn. Reson. Med.*, 2014, **72**, 584.
4. E. S. Roig, A. W. Magill, G. Donati, M. Meyerspeer, L. Xin, O. Ipek, and R. Gruetter, *Magn. Reson. Med.*, 2015, **73**, 894.
5. W. Chen, G. Adriany, X. H. Zhu, R. Gruetter, and K. Ugurbil, *Magn. Reson. Med.*, 1998, **40**, 180.
6. D. E. Befroy, R. J. Perry, N. Jain, S. Dufour, G. W. Cline, J. K. Trimmer, J. Brosnan, D. L. Rothman, K. F. Petersen, and G. I. Shulman, *Nat. Med.*, 2013, **20**, 98.
7. A. Yahya, N. De Zanche, and P. S. Allen, *NMR Biomed.*, 2013, **26**, 533.
8. R. Gruetter, G. Adriany, I. Y. Choi, P. G. Henry, H. Lei, and G. Oz, *NMR Biomed.*, 2003, **16**, 313.
9. R. A. De Graaf, In Vivo NMR Spectroscopy – Principles and Techniques, 2nd edn, John Wiley & Sons: Chichester, England, 2007.
10. N. Beckmann, R. Fried, I. Turkalj, J. Seelig, U. Keller, and G. Stalder, *Magn. Reson. Med.*, 1993, **29**, 583.
11. S. Bluml, J. H. Hwang, A. Moreno, and B. D. Ross, *J. Magn. Reson.*, 2000, **143**, 292.
12. M. Krssak, K. F. Petersen, R. Bergeron, T. Price, D. Laurent, D. L. Rothman, M. Roden, and G. I. Shulman, *J. Clin. Endocrinol. Metab.*, 2000, **85**, 748.
13. D. L. Rothman, I. Magnusson, L. D. Katz, R. G. Shulman, and G. I. Shulman, *Science*, 1991, **254**, 573.
14. A. J. Shaka, J. Keeler, T. Frenkiel, and R. Freeman, *J. Magn. Reson.*, 1983, **52**, 335.
15. M. H. Levitt and R. Freeman, *J. Magn. Reson.*, 1981, **43**, 502.
16. Y. Xiang and J. Shen, *J. Magn. Reson. Imaging*, 2011, **34**, 968.
17. R. Gruetter, G. Adriany, H. Merkle, and P. M. Andersen, *Magn. Reson. Med.*, 1996, **36**, 659.
18. D. E. Befroy, K. F. Petersen, S. Dufour, G. F. Mason, R. A.de Graaf, D. L. Rothman, and G. I. Shulman, *Diabetes*, 2007, **56**, 1376.
19. S. Li, L. An, S. Yu, M. Ferraris Araneta, C. S. Johnson, S. Wang, and J. Shen, *Magn. Reson. Med.*, 2015. doi: 10.1002/mrm.25721. [Epub ahead of print]
20. R. Gruetter, I. Magnusson, D. L. Rothman, M. J. Avison, R. G. Shulman, and G. I. Shulman, *Magn. Reson. Med.*, 1994, **31**, 583.
21. R. Taylor, T. B. Price, D. L. Rothman, R. G. Shulman, and G. I. Shulman, *Magn. Reson. Med.*, 1992, **27**, 13.
22. E. L. Thomas, S. D. Taylor-Robinson, M. L. Barnard, G. Frost, J. Sargentoni, B. R. Davidson, S. C. Cunnane, and J. D. Bell, *Hepatology*, 1997, **25**, 178.
23. E. L. Thomas, J. D. Hanrahan, M. Ala-Korpela, G. Jenkinson, D. Azzopardi, R. A. Iles, and J. D. Bell, *Lipids*, 1997, **32**, 645.
24. J. H. Hwang, S. Bluml, A. Leaf, and B. D. Ross, *NMR Biomed.*, 2003, **16**, 160.
25. I. Dimitrov, J. Ren, D. Douglas, A. D. Sherry, and C. R. Malloy, *Proc. Int. Soc. Magn. Reson. Med.*, 2010, 374.
26. G. Perseghin, P. Scifo, F. De Cobelli, E. Pagliato, A. Battezzati, C. Arcelloni, A. Vanzulli, G. Testolin, G. Pozza, A. Del Maschio, and L. Luzi, *Diabetes*, 1999, **48**, 1600.
27. K. F. Petersen, A. B. West, A. Reuben, D. L. Rothman, and G. I. Shulman, *Hepatology*, 1996, **24**, 114.
28. X. Chen, P. Boesiger, and A. Henning, *NMR Biomed.*, 2013, **26**, 1113.
29. R. A. Jonkers, L. J.van Loon, K. Nicolay, and J. J. Prompers, *Diabetologia*, 2013, **56**, 618.
30. M. Borgs, P. Van Hecke, K. Overloop, C. Decanniere, S. Van Huffel, W. Stalmans, and F. Vanstapel, *NMR Biomed.*, 1993, **6**, 371.
31. R. Gruetter, T. A. Prolla, and R. G. Shulman, *Magn. Reson. Med.*, 1991, **20**, 327.
32. L. H. Zang, M. R. Laughlin, D. L. Rothman, and R. G. Shulman, *Biochemistry*, 1990, **29**, 6815.
33. K. Overloop, P. Van Hecke, F. Vanstapel, H. Chen, S. Van Huffel, A. Knijn, and D.van Ormondt, *NMR Biomed.*, 1996, **9**, 315.
34. D. Laurent, K. E. Schneider, W. K. Prusaczyk, C. Franklin, S. M. Vogel, M. Krssak, K. F. Petersen, H. W. Goforth, and G. I. Shulman, *J. Clin. Endocrinol. Metab.*, 2000, **85**, 2170.
35. T. B. Price, G. Perseghin, A. Duleba, W. Chen, J. Chase, D. L. Rothman, R. G. Shulman, and G. I. Shulman, *Proc. Natl. Acad. Sci. U. S. A.*, 1996, **93**, 5329.
36. P. E. Carey, J. Halliday, J. E. Snaar, P. G. Morris, and R. Taylor, *Am. J. Physiol. Endocrinol. Metab.*, 2003, **284**, E688.
37. M. C. Stephenson, E. Leverton, E. Y. Khoo, S. M. Poucher, L. Johansson, J. A. Lockton, J. W. Eriksson, P. Mansell, P. G. Morris, and I. A. MacDonald, *NMR Biomed.*, 2013, **26**, 1518.
38. S. Rotman, J. Slotboom, R. Kreis, C. Boesch, and E. Jequier, *MAGMA*, 2000, **11**, 114.
39. T. B. Price, D. Laurent, K. F. Petersen, D. L. Rothman, and G. I. Shulman, *J. Appl. Physiol.*, 2000, **88**, 698.
40. M. Zehnder, M. Ith, R. Kreis, W. Saris, U. Boutellier, and C. Boesch, *Med. Sci. Sports Exerc.*, 2005, **37**, 1517.
41. T. Jue, D. L. Rothman, G. I. Shulman, B. A. Tavitian, R. A. Defronzo, and R. G. Shulman, *Proc. Natl. Acad. Sci. U. S. A.*, 1989, **86**, 4489.

42. A. J. Van Den Bergh, C. J. Tack, H. J. Van Den Boogert, G. Vervoort, P. Smits, and A. Heerschap, *Eur. J. Clin. Invest.*, 2000, **30**, 122.
43. G. I. Shulman, D. L. Rothman, T. Jue, P. Stein, R. A. Defronzo, and R. G. Shulman, *N. Engl. J. Med.*, 1990, **322**, 223.
44. G. W. Cline, B. M. Jucker, Z. Trajanoski, A. J. Rennings, and G. I. Shulman, *Am. J. Physiol.*, 1998, **274**, E381.
45. G. W. Cline, K. F. Petersen, M. Krssak, J. Shen, R. S. Hundal, Z. Trajanoski, S. Inzucchi, A. Dresner, D. L. Rothman, and G. I. Shulman, *N. Engl. J. Med.*, 1999, **341**, 240.
46. R. Roussel, P. G. Carlier, J. J. Robert, G. Velho, and G. Bloch, *Proc. Natl. Acad. Sci. U. S. A.*, 1998, **95**, 1313.
47. R. Roussel, P. G. Carlier, C. Wary, G. Velho, and G. Bloch, *Magn. Reson. Med.*, 1997, **37**, 821.
48. R. Roussel, G. Velho, P. G. Carlier, L. Jouvensal, and G. Bloch, *Am. J. Physiol.*, 1996, **271**, E434.
49. V. Lebon, S. Dufour, K. F. Petersen, J. Ren, B. M. Jucker, L. A. Slezak, G. W. Cline, D. L. Rothman, and G. I. Shulman, *J. Clin. Invest.*, 2001, **108**, 733.
50. K. F. Petersen, D. Befroy, S. Dufour, J. Dziura, C. Ariyan, D. L. Rothman, L. DiPietro, G. W. Cline, and G. I. Shulman, *Science*, 2003, **300**, 1140.
51. K. F. Petersen, S. Dufour, and G. I. Shulman, *PLoS Med.*, 2005, **2**, e233.
52. D. L. Rothman, I. Magnusson, G. Cline, D. Gerard, C. R. Kahn, R. G. Shulman, and G. I. Shulman, *Proc. Natl. Acad. Sci. U. S. A.*, 1995, **92**, 983.
53. K. F. Petersen, R. Hendler, T. Price, G. Perseghin, D. L. Rothman, N. Held, J. M. Amatruda, and G. I. Shulman, *Diabetes*, 1998, **47**, 381.
54. G. Perseghin, T. B. Price, K. F. Petersen, M. Roden, G. W. Cline, K. Gerow, D. L. Rothman, and G. I. Shulman, *N. Engl. J. Med.*, 1996, **335**, 1357.
55. K. F. Petersen, M. Krssak, S. Inzucchi, G. W. Cline, S. Dufour, and G. I. Shulman, *Diabetes*, 2000, **49**, 827.
56. M. Krebs, M. Krssak, P. Nowotny, D. Weghuber, S. Gruber, V. Mlynarik, M. Bischof, H. Stingl, C. Furnsinn, W. Waldhausl, and M. Roden, *J. Clin. Endocrinol. Metab.*, 2001, **86**, 2153.
57. M. Roden, M. Krssak, H. Stingl, S. Gruber, A. Hofer, C. Furnsinn, E. Moser, and W. Waldhausl, *Diabetes*, 1999, **48**, 358.
58. M. Roden, T. B. Price, G. Perseghin, K. F. Petersen, D. L. Rothman, G. W. Cline, and G. I. Shulman, *J. Clin. Invest.*, 1996, **97**, 2859.
59. M. C. Delmas-Beauvieux, B. Quesson, E. Thiaudiere, J. L. Gallis, P. Canioni, and H. Gin, *Diabetes*, 1999, **48**, 327.
60. M. Krebs, M. Krssak, E. Bernroider, C. Anderwald, A. Brehm, M. Meyerspeer, P. Nowotny, E. Roth, W. Waldhausl, and M. Roden, *Diabetes*, 2002, **51**, 599.
61. S. Jacob, J. Machann, K. Rett, K. Brechtel, A. Volk, W. Renn, E. Maerker, S. Matthaei, F. Schick, C. D. Claussen, and H. U. Haring, *Diabetes*, 1999, **48**, 1113.
62. M. Krssak, K. Falk Petersen, A. Dresner, L. DiPietro, S. M. Vogel, D. L. Rothman, M. Roden, and G. I. Shulman, *Diabetologia*, 1999, **42**, 113.
63. C. Thamer, J. Machann, O. Bachmann, M. Haap, D. Dahl, B. Wietek, O. Tschritter, A. Niess, K. Brechtel, A. Fritsche, C. Claussen, S. Jacob, F. Schick, H. U. Haring, and M. Stumvoll, *J. Clin. Endocrinol. Metab.*, 2003, **88**, 1785.
64. J. J. Prompers, J. A. Jeneson, M. R. Drost, C. C. Oomens, G. J. Strijkers, and K. Nicolay, *NMR Biomed.*, 2006, **19**, 927.
65. P. Kishore, I. Gabriely, M. H. Cui, J. Di Vito, S. Gajavelli, J. H. Hwang, and H. Shamoon, *Diabetes*, 2006, **55**, 659.
66. G. I. Shulman, D. L. Rothman, Y. Chung, L. Rossetti, W. A.Petit Jr, E. J. Barrett, and R. G. Shulman, *J. Biol. Chem.*, 1988, **263**, 5027.
67. M. Krssak, A. Brehm, E. Bernroider, C. Anderwald, P. Nowotny, M. C. Dalla, C. Cobelli, G. W. Cline, G. I. Shulman, W. Waldhausl, and M. Roden, *Diabetes*, 2004, **53**, 3048.
68. I. Magnusson, D. L. Rothman, B. Jucker, G. W. Cline, R. G. Shulman, and G. I. Shulman, *Am. J. Physiol.*, 1994, **266**, E796.
69. K. F. Petersen, M. Krssak, V. Navarro, V. Chandramouli, R. Hundal, W. C. Schumann, B. R. Landau, and G. I. Shulman, *Am. J. Physiol.*, 1999, **276**, E529.
70. M. Roden, G. Perseghin, K. F. Petersen, J. H. Hwang, G. W. Cline, K. Gerow, D. L. Rothman, and G. I. Shulman, *J. Clin. Invest.*, 1996, **97**, 642.
71. L. H. Nilsson and E. Hultman, *Scand. J. Clin. Lab. Invest.*, 1973, **32**, 325.
72. K. F. Petersen, D. Laurent, D. L. Rothman, G. W. Cline, and G. I. Shulman, *J. Clin. Invest.*, 1998, **101**, 1203.
73. R. Taylor, I. Magnusson, D. L. Rothman, G. W. Cline, A. Caumo, C. Cobelli, and G. I. Shulman, *J. Clin. Invest.*, 1996, **97**, 126.
74. M. Krssak and M. Roden, *Rev. Endocr. Metab. Disord.*, 2004, **5**, 127.
75. J. H. Hwang, G. Perseghin, D. L. Rothman, G. W. Cline, I. Magnusson, K. F. Petersen, and G. I. Shulman, *J. Clin. Invest.*, 1995, **95**, 783.
76. P. E. Thelwall, A. Y. Yemin, T. L. Gillian, N. E. Simpson, M. S. Kasibhatla, Z. N. Rabbani, J. M. Macdonald, S. J. Blackband, and M. P. Gamcsik, *Cancer Res.*, 2005, **65**, 10149.
77. J. T. Skamarauskas, F. Oakley, F. E. Smith, C. Bawn, M. Dunn, D. S. Vidler, M. Clemence, P. G. Blain, R. Taylor, M. P. Gamcsik, and P. E. Thelwall, *Hepatology*, 2013, **59**, 2321.
78. M. G. Bischof, E. Bernroider, M. Krssak, M. Krebs, H. Stingl, P. Nowotny, C. Yu, G. I. Shulman, W. Waldhausl, and M. Roden, *Diabetes*, 2002, **51**, 49.
79. M. G. Bischof, M. Krssak, M. Krebs, E. Bernroider, H. Stingl, W. Waldhausl, and M. Roden, *Diabetes*, 2001, **50**, 392.
80. R. S. Hundal, M. Krssak, S. Dufour, D. Laurent, V. Lebon, V. Chandramouli, S. E. Inzucchi, W. C. Schumann, K. F. Petersen, B. R. Landau, and G. I. Shulman, *Diabetes*, 2000, **49**, 2063.
81. P. Singhal, A. Caumo, P. E. Carey, C. Cobelli, and R. Taylor, *Am. J. Physiol. Endocrinol. Metab.*, 2002, **283**, E275.
82. G. Velho, K. F. Petersen, G. Perseghin, J. H. Hwang, D. L. Rothman, M. E. Pueyo, G. W. Cline, P. Froguel, and G. I. Shulman, *J. Clin. Invest.*, 1996, **98**, 1755.
83. R. Sinha, S. Dufour, K. F. Petersen, V. Lebon, S. Enoksson, Y. Z. Ma, M. Savoye, D. L. Rothman, G. I. Shulman, and S. Caprio, *Diabetes*, 2002, **51**, 1022.
84. M. Roden, H. Stingl, V. Chandramouli, W. C. Schumann, A. Hofer, B. R. Landau, P. Nowotny, W. Waldhausl, and G. I. Shulman, *Diabetes*, 2000, **49**, 701.
85. H. Stingl, M. Krssak, M. Krebs, M. G. Bischof, P. Nowotny, C. Furnsinn, G. I. Shulman, W. Waldhausl, and M. Roden, *Diabetologia*, 2001, **44**, 48.
86. M. Krebs, A. Brehm, M. Krssak, C. Anderwald, E. Bernroider, P. Nowotny, E. Roth, V. Chandramouli, B. R. Landau, W. Waldhausl, and M. Roden, *Diabetologia*, 2003, **46**, 917.
87. D. L. Rothman, K. L. Behar, F. Hyder, and R. G. Shulman, *Annu. Rev. Physiol.*, 2003, **65**, 401.
88. S. Ramadan, A. Lin, and P. Stanwell, *NMR Biomed.*, 2013, **26**, 1630.
89. P. Morris and H. Bachelard, *NMR Biomed.*, 2003, **16**, 303.
90. R. A.de Graaf, G. F. Mason, A. B. Patel, K. L. Behar, and D. L. Rothman, *NMR Biomed.*, 2003, **16**, 339.
91. R. A.de Graaf, D. L. Rothman, and K. L. Behar, *NMR Biomed.*, 2011, **24**, 958.
92. A. B. Criego, I. Tkac, A. Kumar, W. Thomas, R. Gruetter, and E. R. Seaquist, *J. Neurosci. Res.*, 2005, **82**, 525.

93. A. B. Criego, I. Tkac, A. Kumar, W. Thomas, R. Gruetter, and E. R. Seaquist, *J. Neurosci. Res.*, 2005, **79**, 42.
94. I. Y. Choi, S. P. Lee, S. G. Kim, and R. Gruetter, *J. Cereb. Blood Flow Metab.*, 2001, **21**, 653.
95. R. Gruetter, K. Ugurbil, and E. R. Seaquist, *J. Neurochem.*, 1998, **70**, 397.
96. E. R. Seaquist, G. S. Damberg, I. Tkac, and R. Gruetter, *Diabetes*, 2001, **50**, 2203.
97. I. Y. Choi and R. Gruetter, *Neurochem. Int.*, 2003, **43**, 317.
98. I. Y. Choi, E. R. Seaquist, and R. Gruetter, *J. Neurosci. Res.*, 2003, **72**, 25.
99. I. Y. Choi, I. Tkac, K. Ugurbil, and R. Gruetter, *J. Neurochem.*, 1999, **73**, 1300.
100. I. Y. Choi, I. Tkac, and R. Gruetter, *Magn. Reson. Med.*, 2000, **44**, 387.
101. F. D. Morgenthaler, D. M. Koski, R. Kraftsik, P. G. Henry, and R. Gruetter, *Neurochem. Int.*, 2006, **48**, 616.
102. G. Oz, E. R. Seaquist, A. Kumar, A. B. Criego, L. E. Benedict, J. P. Rao, P. G. Henry, P. F. Van de Moortele, and R. Gruetter, *Am. J. Physiol. Endocrinol. Metab.*, 2006, **292**, E946.
103. D. L. Rothman, *NMR Biomed.*, 2001, **14**, 149.
104. R. G. Shulman, D. L. Rothman, K. L. Behar, and F. Hyder, *Trends Neurosci.*, 2004, **27**, 489.
105. R. Gruetter, E. R. Seaquist, and K. Ugurbil, *Am. J. Physiol. Endocrinol. Metab.*, 2001, **281**, E100.
106. V. Lebon, K. F. Petersen, G. W. Cline, J. Shen, G. F. Mason, S. Dufour, K. L. Behar, G. I. Shulman, and D. L. Rothman, *J. Neurosci.*, 2002, **22**, 1523.
107. J. Shen, K. F. Petersen, K. L. Behar, P. Brown, T. W. Nixon, G. F. Mason, O. A. Petroff, G. I. Shulman, R. G. Shulman, and D. L. Rothman, *Proc. Natl. Acad. Sci. U. S. A.*, 1999, **96**, 8235.
108. G. F. Mason, K. F. Petersen, R. A. de Graaf, G. I. Shulman, and D. L. Rothman, *J. Neurochem.*, 2007, **100**, 73.
109. S. Bluml, A. Moreno, J. H. Hwang, and B. D. Ross, *NMR Biomed.*, 2001, **14**, 19.
110. A. Moreno, S. Bluml, J. H. Hwang, and B. D. Ross, *Magn. Reson. Med.*, 2001, **46**, 39.
111. S. Bluml, A. Moreno-Torres, F. Shic, C. H. Nguy, and B. D. Ross, *NMR Biomed.*, 2002, **15**, 1.
112. S. Bluml, A. Moreno-Torres, and B. D. Ross, *Magn. Reson. Med.*, 2001, **45**, 981.
113. A. Moreno, B. D. Ross, and S. Bluml, *J. Neurochem.*, 2001, **77**, 347.
114. W. Chen, X. H. Zhu, R. Gruetter, E. R. Seaquist, G. Adriany, and K. Ugurbil, *Magn. Reson. Med.*, 2001, **45**, 349.
115. G. F. Mason, J. W. Pan, W. J. Chu, B. R. Newcomer, Y. Zhang, R. Orr, and H. P. Hetherington, *J. Cereb. Blood Flow Metab.*, 1999, **19**, 1179.
116. G. F. Mason, P. K. Falk, R. A.de Graaf, T. Kanamatsu, T. Otsuki, G. I. Shulman, and D. L. Rothman, *Brain Res. Protoc.*, 2003, **10**, 181.
117. J. W. Pan, R. A.de Graaf, K. F. Petersen, G. I. Shulman, H. P. Hetherington, and D. L. Rothman, *J. Cereb. Blood Flow Metab.*, 2002, **22**, 890.
118. N. Chhina, E. Kuestermann, J. Halliday, L. J. Simpson, I. A. Macdonald, H. S. Bachelard, and P. G. Morris, *J. Neurosci. Res.*, 2001, **66**, 737.